CHEMISTRY OF MATERIALS

ARTICLE

pubs.acs.org/cm

Ruthenium(II)-Cored Polythiophene Dendrimers

Suxiang Deng, Greg Krueger, Prasad Taranekar, Saengrawee Sriwichai, Ruifa Zong, Randolph P. Thummel, and Rigoberto C. Advincula*

Department of Chemistry and Department of Chemical and Biomolecular Engineering, University of Houston, 4800 Calhoun Road, Houston, Texas 77204-5003, United States

Supporting Information

ABSTRACT: We report the synthesis and characterization of ruthenium(II)-cored polythiophene dendrimers. Four new redox-active ruthenium(II) pyridine oligothiophene dendritic complexes that fluoresce in the near-infrared region have been synthesized, and their absorption spectra, fluorescence properties, and redox behavior have been investigated. The dendritic ligands **phen3T** and **phen7T** containing 1,10-phenanthroline as chelating sites and two oligothiophene dendrons (**3T6COMe** and **7T6COMe**) have been synthesized and employed. The metal−polythiophene dendrimers investigated here are $[Ru(bpy)_2(\mathbf{phen3T})]^{2+}$, $[Ru(bpy)_2(\mathbf{phen7T})]^{2+}$, $[Ru(\mathbf{phen3T})_3]^{2+}$, and $[Ru(\mathbf{phen7T})_3]^{2+}$. Upon addition of acid, the charge transfer absorption bands of free dendritic ligands are significantly red-shifted and the fluorescence is greatly quenched. The Ru(II) polythiophene dendrimers exhibit very strong metal-to-ligand charge transfer (MLCT) absorption and enhanced absorption in the UV region and can be regarded as better light-harvesting species. The MLCT emission is extraordinarily red-shifted (∼165 nm) because of their planar excited states. The core of the dendrimers shows an electrochemical behavior typical of encapsulated metal electroactive units.

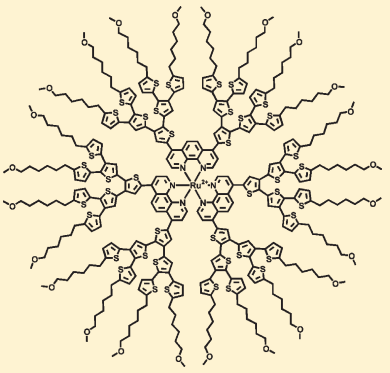

KEYWORDS: oligothiophene, dendrimers, ruthenium, metal-to-ligand charge transfer

INTRODUCTION

Transfer of energy from an antenna unit to a chemically active center has been considered to be a crucial step in photosynthesis.[1] Tremendous efforts have been made to construct molecular systems having such functions. Among a variety of photosynthetic systems, metal-containing dendrimers have been extensively investigated.[2] Dendritic molecules constructed around Ru(II) polypyridyl-type complexes that display metal-to-ligand charge transfer (MLCT) excited states are very intriguing because of their outstanding photochemical, photophysical, and electrochemical properties.[3] Many large dendritic arrays of MLCT complexes show novel photophysical and electrochemical properties;[4] however, larger fused analogues usually suffer from poor solubility and inefficient syntheses.[5]

In the past, our group has reported the synthesis of thiophene dendrons and dendrimers[6] and their interesting two-dimensional supramolecular assembly on graphite.[7] Besides their excellent assembly properties, these thiophene dendrimers also exhibit strong absorption in the region of 250−400 nm and are good light-harvesting macromolecules. Since our group's first report on thiophene dendrimer synthesis, several new types of thiophene dendrimers for applications such as light harvesting, solar energy conversion, and optoelectronics have been reported. Ma et al.[8] have developed an effective approach to synthesizing a series of protected and nonsubstituted thiophene dendrons and dendrimers up to the fourth generation with 90 thiophene units. The potential application of these thiophene dendrimers as an entangled photon sensor has also been explored.[9] Mitchell et al.[10] synthesized phenyl-cored thiophene dendrimers and reported a power conversion efficiency of 1.3% for organic photovoltaic devices based on these dendrimers.[11] Aso et al.[12] have prepared another series of thiophene dendrimers containing quaterthiophene as repeating conjugated bridges and benzene rings as branching centers. Very recently, Wong et al. reported organic solar cells based on hexa-*peri*-hexabenzocoronene-cored thiophene dendrimers having a power conversion efficiency of 2.5%.[13] Other groups have reported various routes.[14] Further details about synthesis, properties, and applications of thiophene dendrimers can be found in the review by Bäuerle, Ma, and Mishra.[15]

Here, we report the synthesis, absorption spectra, redox behavior, and photophysical properties of metal-cored polythiophene dendrimers and oligothiophene dendritic polypyridine ligands. The dendritic ligands are termed **phen3T** and **phen7T** (Scheme 1), combining a 1,10-phenanthroline chelating site with two oligothiophene dendrons (**3T6COMe** and **7T6COMe**). The corresponding metal dendrimers $[Ru(bpy)_2(\mathbf{phen3T})]^{2+}$, $[Ru(bpy)_2(\mathbf{phen7T})]^{2+}$, $[Ru(\mathbf{phen3T})_3]^{2+}$, and $[Ru(\mathbf{phen7T})_3]^{2+}$ were also investigated (Scheme 2). Oligothiophene dendrons in these ligands and metal complexes provide good solubility, extended conjugation for 1,10-phenanthroline, and a large cross section for photon collection, a feature particularly suited to light harvesting.

Received: January 22, 2011
Revised: May 21, 2011
Published: June 22, 2011

Scheme 1. Synthesis Steps for Dendritic Ligands phen3T and phen7T

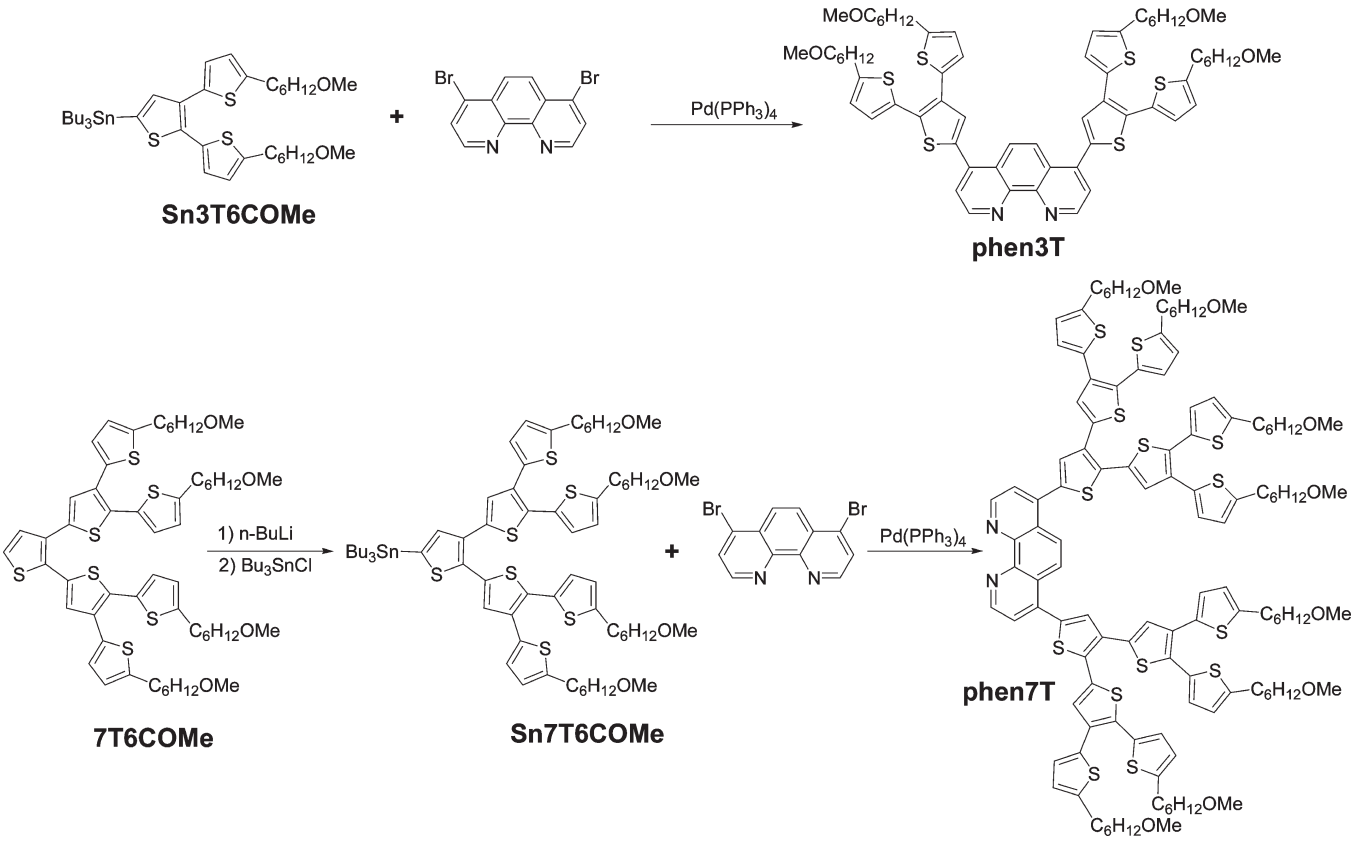

RESULTS AND DISCUSSION

Synthesis and Structural Characterization of Oligothiophene Dendrons, Dendritic Ligands, and Ru(II) Complexes. Thiophene dendrons and their corresponding tri-*n*-butyltin derivatives (**Sn3T6COMe** and **Sn7T6COMe**) were synthesized by procedures similar to those reported previously.[6] Compared with the synthesis of thiophene dendrons having only hexyl chains, the introduction of the methoxyhexyl group makes separation of the thiophene dendrons easier because of the larger polarity difference between lower- and higher-generation thiophene dendrons. For instance, the difference in the R_f values of **3T6C** and **7T6C** is only 0.14 (0.47 for **3T6C** vs 0.33 for **7T6C**) even when the best eluent (10:1 hexane/CH_2Cl_2, v/v) for separation is used. On the other hand, the difference in the R_f values of **3T6COMe** and **7T6COMe** is 0.27 (0.43 for **3T6COMe** vs 0.16 for **7T6COMe**) with a 1:1 (v/v) hexane/diethyl ether mixture as the eluent. Moreover, the terminal hexyl methoxide groups made possible the separation of the doubly coupled product **phen7T** from the monocoupled byproduct **Brphen7T** (see the Supporting Information) because the difference in the R_f values of **phen7T** and **Brphen7T** is as large as 0.28 with a 20:1 (v/v) CH_2Cl_2/CH_3OH mixture as the eluent. With only hexyl chains, there is almost no difference in R_f values, although various eluents have been tried. From ^{1}H nuclear magnetic resonance (NMR), it was very clear that both a doubly coupled product and a monocoupled byproduct were obtained. However, attempts to separate them were not successful.

The dendritic ligands **phen3T** and **phen7T** were synthesized by Stille coupling of 4,7-dibromo-1,10-phenanthroline with tri-*n*-butyltin derivatives of the thiophene dendrons **3T6COMe** and **7T6COMe**, respectively (Scheme 1). It is worth pointing out that at least 10 mol % $Pd(PPh_3)_4$ must be used to achieve high reaction yields because 4,7-dibromo-1,10-phenanthroline will partially poison the catalyst,[16] thus decreasing its catalytic activity. The reaction yield decreases as the dendron size increases. For **3T6COMe**, only a trace of monocoupled byproduct was observed by TLC. However, for **7T6COMe**, the monocoupled byproduct **Brphen7T** was separated and its structure was confirmed by NMR.

The metal complexes $[Ru(bpy)_2(\mathbf{phen3T})]^{2+}$, $[Ru(bpy)_2(\mathbf{phen7T})]^{2+}$, $[Ru(\mathbf{phen3T})_3]^{2+}$, and $[Ru(\mathbf{phen7T})_3]^{2+}$ were prepared by treating $[Ru(bpy)_2Cl_2]$ or $[RuCl_3]$ with the appropriate ligands.[17,18] The redox behavior, absorption, and fluorescence spectra of dendritic ligands and their metal complexes have been studied. For comparison, two model complexes, $[Ru(bpy)_2(phen)]^{2+}$ and $[Ru(phen)_3]^{2+}$, were also synthesized, and their properties were studied. Except for $[Ru(\mathbf{phen7T})_3]^{2+}$, the structures of all metal complexes were confirmed by MALDI-MS and ^{1}H and ^{13}C NMR spectroscopy (see the Supporting Information).

Free Ligands Subjected to Absorption Spectroscopy. Both **phen3T** and **phen7T** show strong absorption in the 240−400 nm region and weak absorption in the 400−500 nm region (see Figure 1). The strong absorption bands in the 290−400 nm region are associated with ligand-centered transitions, whereas the weak absorptions in the 400−500 nm region are due to thiophene dendron-to-phenanthroline charge transfer transitions. Both **phen3T** and **phen7T** show two strong absorption bands at ∼242 and ∼288 nm (Figure 1 and Table 1). The band at

dx.doi.org/10.1021/cm200228p |*Chem. Mater.* 2011, 23, 3302–3311

Scheme 2. Synthesis Steps for the Final Ru Metal−Dendron Complexes

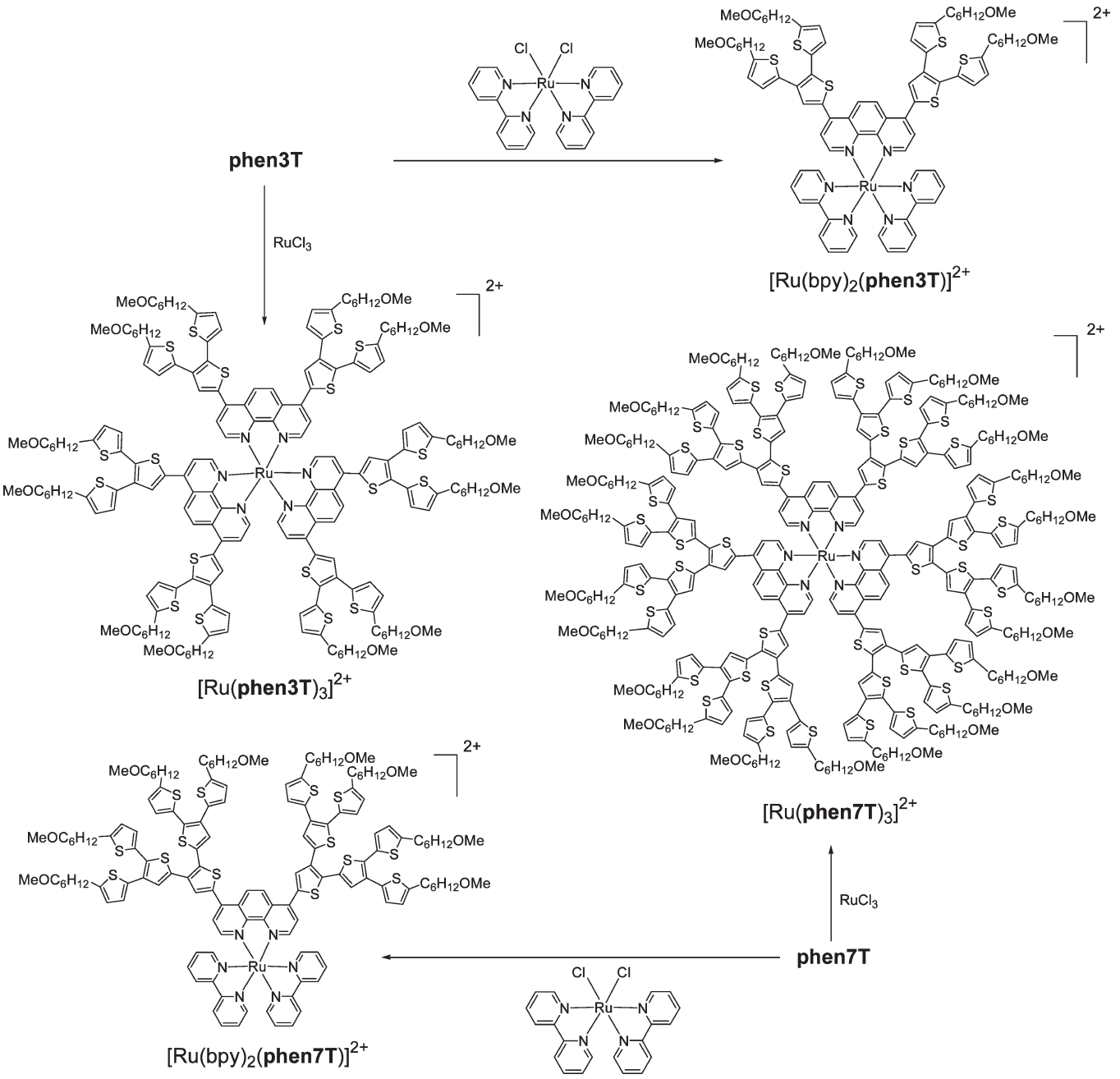

~242 nm, which is already present in thiophene dendrons **3T6COMe** and **7T6COMe**, is associated with thiophene-centered transitions. Although contributions from thiophene-centered transitions are not negligible, the band with a maximum at ~288 nm is more likely from a phenanthroline-centered transition, which is red-shifted from the parent phenanthroline (λ_{max} = 260 nm) because of the conjugation provided by thiophene dendrons. Dendritic ligand **phen3T** also displays an absorption shoulder at ~370 nm, which is most likely a combination of red-shifted thiophene dendron-centered transitions and thiophene dendron-to-phenanthroline charge transfer transitions. This assignment is further supported by changes in the absorption spectra of **phen3T** upon addition of acid (Figure 2). The presence of the acid results in relatively intense bands in the 400−600 nm range. For example, an absorption shoulder at ~470 nm appears in the absorption spectrum of **phen3T**, and a broad band that extends to 650 nm appears in the absorption spectrum of **phen7T**. These new bands can be explained by a red shift of the thiophene dendron-to-phenanthroline charge transfer (CT) transitions, as a consequence of stabilization of the phenanthroline-based acceptor orbitals upon protonation, probably with concomitant enhancement of the oscillator strength of the CT transitions.[19] The bands at wavelengths of <350 nm for **phen3T** and <450 nm for **phen7T**, on the other hand, are only weakly affected by protonation. Therefore, the contribution of CT transitions to these absorption bands is negligible.

Metal Complexes Subjected to Absorption Spectroscopy. The absorption spectra of the metal complexes are dominated by

dx.doi.org/10.1021/cm200228p |*Chem. Mater.* 2011, 23, 3302–3311

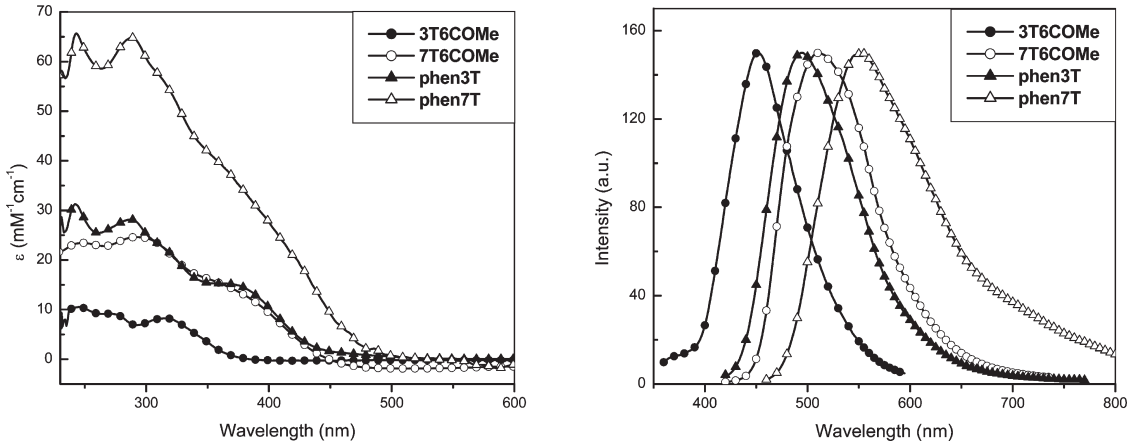

Figure 1. Absorption (left) and emission (right) spectra of thiophene dendrons (**3T6COMe** and **7T6COMe**) and dendritic ligands (**phen3T** and **phen7T**).

Table 1. Extinction Coefficients, Absorption, and Emission Maxima

compd	λ^{abs}_{max} (nm) (log ε)[a]	λ^{fl}_{max} (nm)[b]
3T6COMe	245 (4.02), 272sh (3.96), 316 (3.92)	452
7T6COMe	248 (4.37), 293 (4.39), 375sh (4.13)	511
phen3T	242 (4.50), 288 (4.45), 370sh (4.18)	495
phen7T	243 (4.82), 288 (4.81)	554
$[Ru(bpy)_2(phen)]^{2+}$	266 (4.72), 287 (4.76), 451 (4.17)	599
$[Ru(bpy)_2(\mathbf{phen3T})]^{2+}$	243 (4.65), 288 (4.90), 335sh (4.41), 458 (4.48)	734
$[Ru(bpy)_2(\mathbf{phen7T})]^{2+}$	243 (4.85), 289 (5.02), 443 (4.52)	615
$[Ru(phen)_3]^{2+}$	264 (5.04), 446 (4.25)	581
$[Ru(\mathbf{phen3T})_3]^{2+}$	242 (5.01), 282 (5.11), 335sh (4.87), 473 (4.86)	747
$[Ru(\mathbf{phen7T})_3]^{2+}$	244 (5.30), 284 (5.32), 475sh (4.85)	634

[a] For the absorption, the maxima (or shoulders) of the relevant bands are given. [b] Maxima obtained from uncorrected emission spectra. λ_{ex} = 450 nm with CH_2Cl_2 as the solvent.

intense UV bands and by moderately intense bands in the visible region (Figure 3). The UV bands are assigned to spin-allowed ligand-centered (LC) transitions, and the visible bands are attributed to spin-allowed metal-to-ligand charge transfer (MLCT) transitions, similar to those of other Ru(II)−polypyridine complexes.[20] Both model complexes $[Ru(bpy)_2(phen)]^{2+}$ and $[Ru(phen)_3]^{2+}$ show a phenanthroline-centered absorption band at ~265 nm (Figure 3 and Table 1). The band at ~288 nm, which is present in all dendritic species, is attributed to LC transitions involving the delocalized phenanthroline moiety (**phen3T** or **phen7T**). The dendritic species $[Ru(bpy)_2(\mathbf{phen3T})]^{2+}$, $[Ru(bpy)_2(\mathbf{phen7T})]^{2+}$, $[Ru(\mathbf{phen3T})_3]^{2+}$, and $[Ru(\mathbf{phen7T})_3]^{2+}$ exhibit enhanced absorption around 240 nm and in the region 300−350 nm compared to the reference complexes $[Ru(bpy)_2(phen)]^{2+}$ and $[Ru(phen)_3]^{2+}$. These latter features can be safely assigned to transitions involving the thiophene dendrons. In further support of this assignment, the size of these absorption bands increased with the size of the thiophene dendrons.

For the model complex $[Ru(bpy)_2(phen)]^{2+}$, the band at 451 nm arises from Ru(II)-to-bpy transitions, while the band at ~446 nm for $[Ru(phen)_3]^{2+}$ arises from Ru(II)-to-phenanthroline transitions. The absorption band of $[Ru(\mathbf{phen3T})_3]^{2+}$ at ~475 nm can be assigned to a typical MLCT state involving a metal d orbital and the π^* orbital of a ligand (**phen3T**). For the extended organic π systems, it is well-known that as the degree of conjugation increases, the π^* orbitals are stabilized,[21] which results in a red shift of the lowest-energy absorption band. In the same way, it appears that the 27 nm shift of the MLCT absorption maxima from $[Ru(phen)_3]^{2+}$ to $[Ru(\mathbf{phen3T})_3]^{2+}$ suggests an increased level of conjugation (i.e., delocalization) in $[Ru(\mathbf{phen3T})_3]^{2+}$. The broad and red-shifted MLCT absorption band of $[Ru(bpy)_2(\mathbf{phen3T})]^{2+}$ is likely a combination of dπ(Ru)-to-π^*(bpy) and dπ(Ru)-to-π^*(**phen3T**) transitions. Similarly, the MLCT band of $[Ru(bpy)_2(\mathbf{phen7T})]^{2+}$ is a combination of dπ(Ru)-to-π^*(bpy) and dπ(Ru)-to-π^*(**phen7T**) transitions. Because of the increased ligand-centered absorption in the UV region, $[Ru(\mathbf{phen7T})_3]^{2+}$ shows only a MLCT absorption shoulder at ~475 nm, which makes it difficult to compare the relative conjugation effect of the thiophene dendron **7T6COMe**.

The MLCT bands of $[Ru(bpy)_2(\mathbf{phen3T})]^{2+}$, $[Ru(bpy)_2(\mathbf{phen7T})]^{2+}$, $[Ru(\mathbf{phen3T})_3]^{2+}$, and $[Ru(\mathbf{phen7T})_3]^{2+}$ are broader and red-shifted in comparison with those of $[Ru(bpy)_2(phen)]^{2+}$ and $[Ru(phen)_3]^{2+}$. Moreover, the intensities of MLCT bands of dendritic metal complexes are much stronger. As a consequence, ruthenium thiophene dendrimers can be regarded as better light-harvesting species than the model Ru(II) complexes, because they display enhanced absorption in a region where the absorption of the model compounds is poor (the 300−360 nm region) and also their absorption spectra extend more toward the red.

dx.doi.org/10.1021/cm200228p |*Chem. Mater.* 2011, 23, 3302–3311

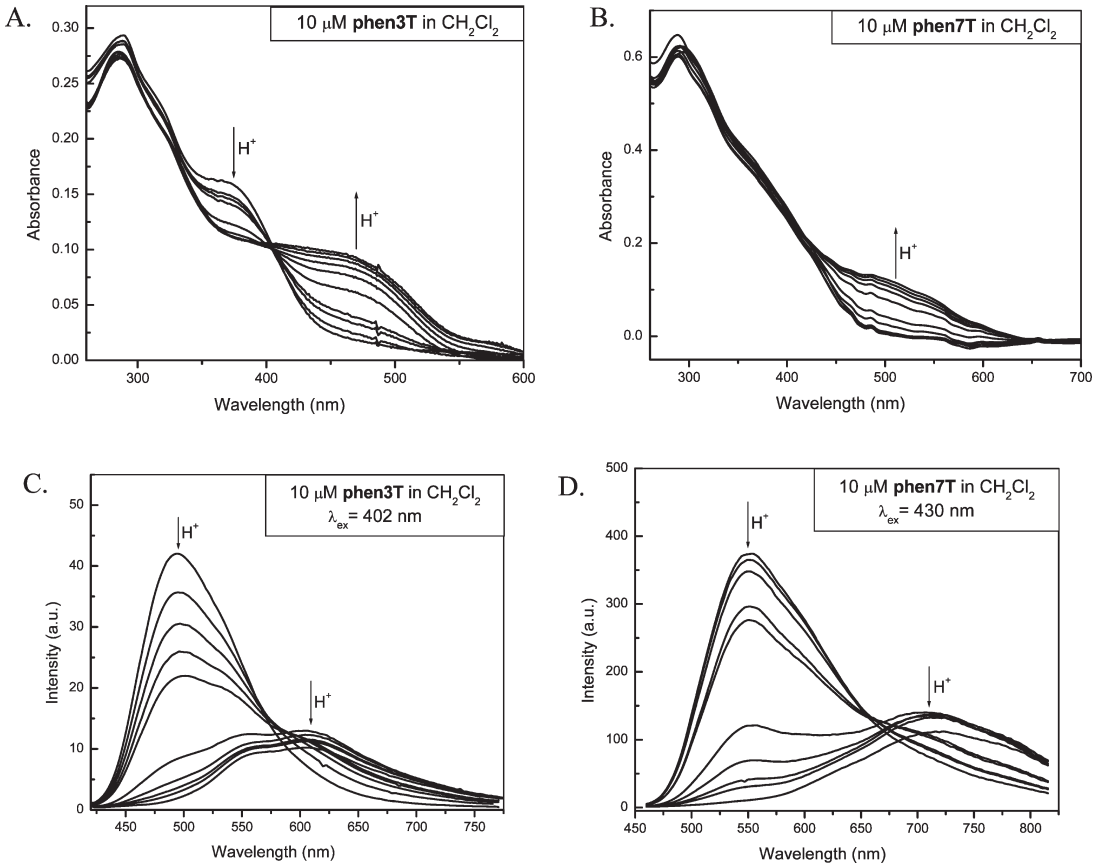

Figure 2. Effect of added CF_3COOH on the absorption spectra of **phen3T** (A) and **phen7T** (B) and the emission spectra of **phen3T** (C) and **phen7T** (D). The excitation wavelength was the isosbestic point. Samples were prepared by mixing 0, 10, 20, 30, 40, 80, 120, 160, 200, and 400 μL of the CF_3COOH solution (0.1 mM) with a **phen3T** or **phen7T** solution (2.0 mL, 10 μM).

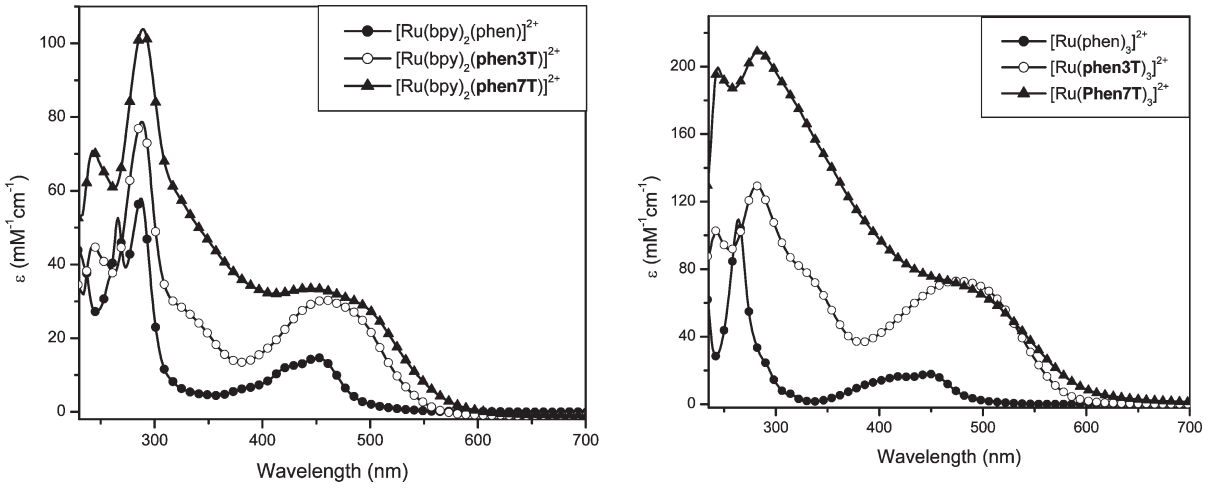

Figure 3. Optical absorption spectra of metal complexes (~10 μM in CH_2Cl_2).

Free Ligands Subjected to Fluorescence Spectroscopy. Though the luminescence spectra of **phen3T** and **phen7T** are red-shifted and slightly broadened when compared with those of **3T6COMe** and **7T6COMe**, they can still be assigned to the lowest-lying $\pi-\pi^*$ singlet level of the thiophene dendrons. The fluorescence tail at longer wavelengths is attributed to CT (thiophene dendron to phenanthroline) excited states as confirmed by the change in the fluorescence spectra upon addition of acid (Figure 2).

For **phen3T**, the intensity of emission at ~495 nm decreases as more acid is added. An emission peak at ~605 nm and a shoulder at ~560 nm appear when 0.4 molar equiv of CF_3COOH (80 μL of a 0.1 mM solution) is added. The intensity of these two emission bands also decreases as the concentration

dx.doi.org/10.1021/cm200228p |*Chem. Mater.* 2011, 23, 3302–3311

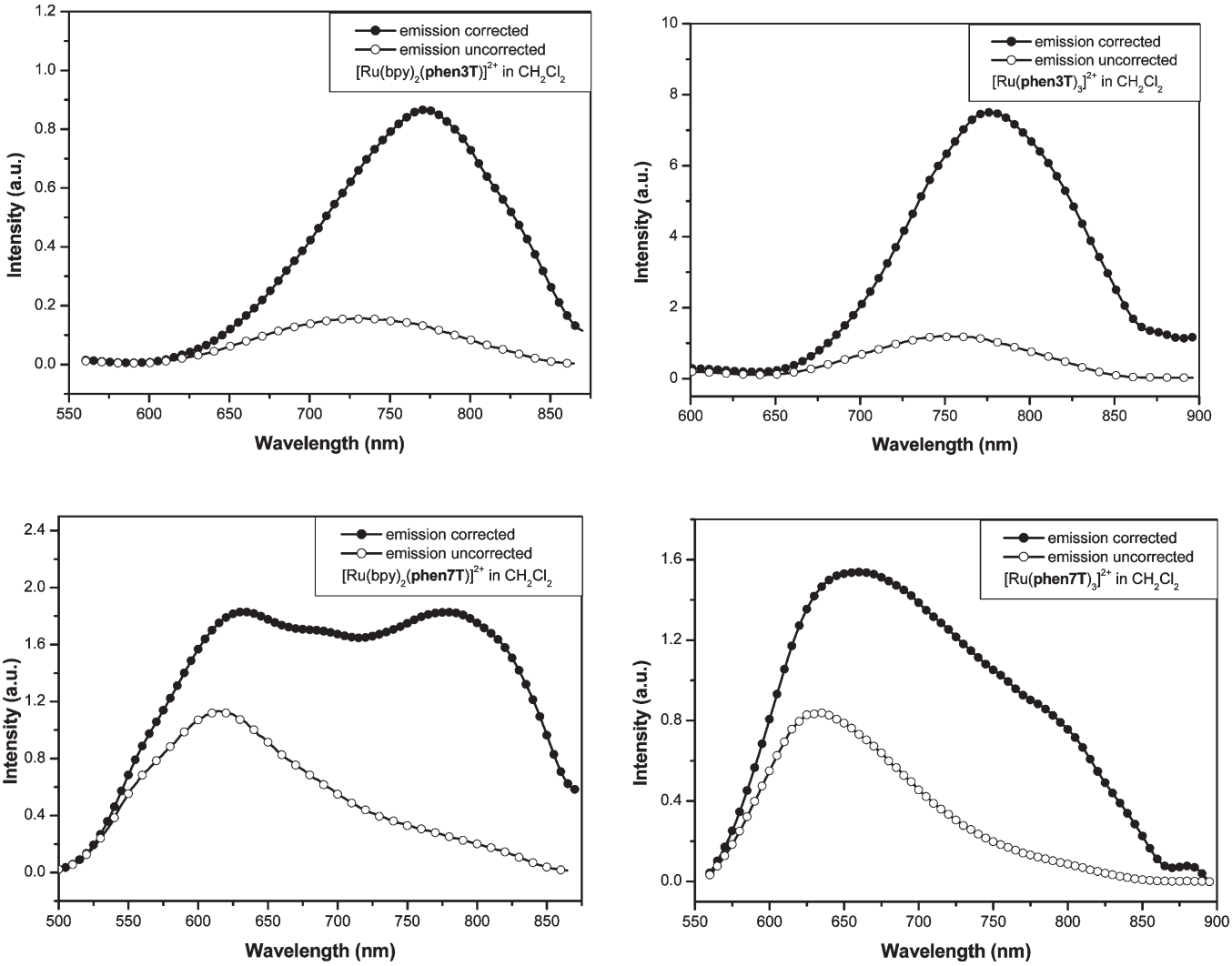

Figure 4. Emission spectra of metal complexes (λ_{ex}= 450 nm). The concentration was approximately 10 μM.

of acid increases, but their intensities are not as sensitive as that of the emission at ~495 nm.

Dendritic ligand **phen7T** shows a similar emission behavior upon addition of acid. The intensity of the emission at ~550 nm decreases as more acid is added. A new emission band at ~705 nm appears when 0.4 molar equiv of CF_3COOH is added. The intensity of the latter emission band also decreases as the concentration of acid increases, but the intensity is not as sensitive as that of the emission at 550 nm.

However, ~25% fluorescence intensity remains even in the presence of a large excess of acid (up to 100 molar equiv). Because of their relatively intense luminescence, the dendritic ligands **phen3T** and **phen7T** can also be regarded as luminescent sensors, taking advantage of their free coordination/protonatable sites. Indeed, protonation of either **phen3T** or **phen7T** results in a red-shifted absorption and luminescence bands.

Metal Complexes Subjected to Fluorescence Spectroscopy. It is clear that the ruthenium−polythiophene dendrimers fluoresce in the near-IR region (Figure 4 and Table 1). Both corrected and uncorrected spectra are shown (Supporting Information) with the discussions based on the corrected spectra. The emission of the model complex $[Ru(phen)_3]^{2+}$ (λ^{fl}_{max} = 581 nm) originates from a Ru-to-phenanthroline CT state. Similarly, the emission of $[Ru(\mathbf{phen3T})_3]^{2+}$ centered around 747 nm can be assigned to the Ru-to-**phen3T** CT state. This unusually large red shift (~165 nm)

Table 2. Cyclic Voltammety Data[a]

compd	$E_{1/2}^{ox}$ (ΔE)	$E_{1/2}^{red}$ (ΔE)
ferrocene	0.50 (151)	
phen3T		-0.66^{ir}
phen7T		-0.68^{ir}
$[Ru(bpy)_2(phen)]^{2+}$	1.51 (102)	−1.23 (98), −1.48 (153)
$[Ru(bpy)_2(\mathbf{phen3T})]^{2+}$	1.46 (221)	-1.21^{ir}, -1.57^{ir}
$[Ru(bpy)_2(\mathbf{phen7T})]^{2+}$		-1.31^{ir}
$[Ru(phen)_3]^{2+}$	1.49 (137)	−1.27 (112), −1.46 (196), −1.80 (122)
$[Ru(\mathbf{phen3T})_3]^{2+}$	1.41 (285)	-1.17^{ir}, -1.41^{ir}
$[Ru(\mathbf{phen7T})_3]^{2+}$		

[a] Recorded in CH_2Cl_2 containing 0.05 M NBu_4PF_6; $E_{1/2}$ in volts vs SCE and ΔE in millivolts; scan rate of 100 mV/s.

dx.doi.org/10.1021/cm200228p |*Chem. Mater.* 2011, 23, 3302–3311

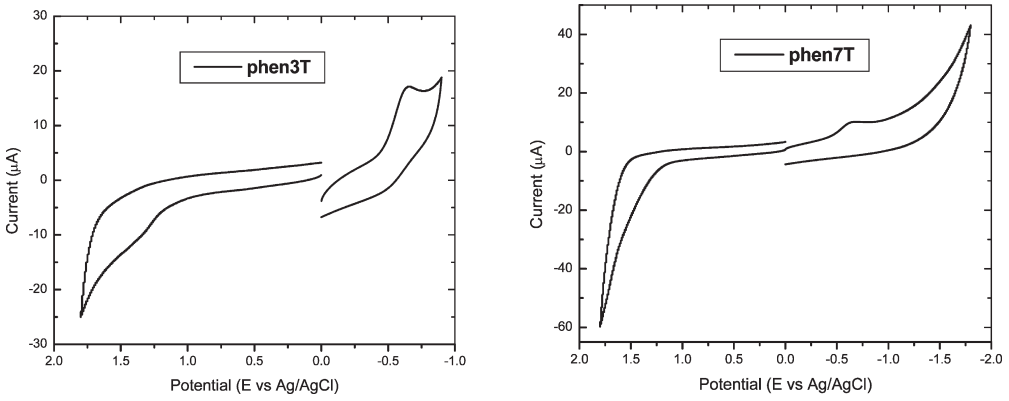

Figure 5. Cyclic voltammograms of dendritic oligothiophene ligands **phen3T** and **phen7T**.

indicates that the thiophene dendron **3T6COMe** has very strong electronic interactions with Ru-to-phenanthroline CT states and strongly stabilizes these MLCT states. A large red shift (~135 nm) was also observed in the emission of $[Ru(bpy)_2(\mathbf{phen3T})]^{2+}$. McCusker et al.[18] studied the delocalization effect of the peripheral phenyl group and its subsequent effect on the photophysical properties of a series of aryl-substituted 2,2′-bipyridyl Ru(II) complexes. They proved that the unusual photophysical properties of $[Ru(4,4'\text{-diphenyl-2,2}'\text{-bipyridine})_3](PF_6)_2$ are caused by the coplanarity of the bipyridyl and phenyl fragments in the excited state and nonplanarity in the ground state. We believe that **3T6COMe** thiophene dendrons rotate into the plane of the bpy ligand to form a planar configuration in the excited state. This planarity leads to an efficient intraligand delocalization in the MLCT excited state, resulting in an abnormally large bathochromic shift. As the size of thiophene dendrons increases, the steric bulk strongly hinders coplanarity, correspondingly attenuating intraligand delocalization. An ~50 nm bathochromic shift is observed in the emission of $[Ru(\mathbf{phen7T})_3]^{2+}$ though.

Because of the unusually large bathochromic shift observed in the emission, these ruthenium−thiophene dendrimers are very intriguing in terms of photophysical properties, although it is not fully understood at present why the ruthenium−thiophene dendrimer $[Ru(bpy)_2(\mathbf{phen3T})]^{2+}$ shows an only ~15 nm red shift. While coplanarity alone is probably not enough for attribution of these unusually large bathochromic shifts, other factors such as packing between thiophene dendrons might also play an important role. More photophysical investigations will be needed to fully understand these interesting dendrimers, including fluorescence lifetime measurements.

Redox Behavior. The redox data of the investigated metal complexes and dendritic ligands are listed in Table 2, as reported against the SCE reference, and also are shown in Figure S2 of the Supporting Information. Ferrocene was used to calibrate the reference electrode and its half-oxidation potential was 0.5 V versus SCE. Both dendritic ligands **phen3T** and **phen7T** show an ill-defined and mainly irreversible CV response (Figure 5). Only an irreversible reduction peak centered at approximately −0.7 V is observable. No distinguishable oxidation peak can be found.

For the assignment of the electrochemical processes of the dendritic metal complexes, the CV data of two model complexes, $[Ru(bpy)_2(phen)]^{2+}$ and $[Ru(phen)_3]^{2+}$, are also listed in Table 2. $[Ru(bpy)_2(phen)]^{2+}$ shows two reversible ligand-centered reductions and a reversible oxidation of Ru(II)/Ru(III),[19,22] while $[Ru(phen)_3]^{2+}$ exhibits three reversible ligand reductions and a reversible metal-centered oxidation (Figure S2 of the Supporting Information).[23] Compared with $[Ru(bpy)_2(phen)]^{2+}$, the heteroleptic complex $[Ru(bpy)_2(\mathbf{phen3T})]^{2+}$ has a less positive oxidation potential at 1.46 V (Table 2 and Figure 6). Oxidation involves the removal of one electron from the metal d orbital. Thus, the d orbital of ruthenium was destabilized by the ligand **phen3T**. As previously shown by Thummel et al.,[24] electron-donating groups such as NMe_2 on 2,2′-bipyridine destabilize the HOMO ($d\pi$) of the metal. Therefore, thiophene dendrons **3T6COMe** on dendritic ligand **phen3T** act as electron-donating groups due to conjugation with 1,10-phenanthroline. The destabilization effect of **phen3T** on the ruthenium d orbital is even more prominent in the homoleptic dendritic complex $[Ru(\mathbf{phen3T})_3]^{2+}$. A typical electroactive Ru(II) metallodendrimer has a more positive oxidation potential than nondendritic analogues because of site-isolation/encapsulation effects.[25,26] A less positive oxidation potential observed in $[Ru(\mathbf{phen3T})_3]^{2+}$ (Table 2) is definitely due to the destabilization effect of the dendritic ligand **phen3T**. On the other hand, $[Ru(\mathbf{phen3T})_3]^{2+}$ shows reduction at a potential less negative than that observed in $[Ru(phen)_3]^{2+}$, which is typical of the reduction behavior of electroactive Ru(II) metallodendrimers.[26] Therefore, for $[Ru(\mathbf{phen3T})_3]^{2+}$, the HOMO (ruthenium d orbital) is destabilized and the LUMO (π^* orbital of the ligand) is stabilized. The combination of these two effects should lead to this abnormally large (~170 nm) red-shifted fluorescence observed in $[Ru(\mathbf{phen3T})_3]^{2+}$.

Unfortunately, it is difficult to locate the exact oxidation and reduction potentials because of the irreversible electrochemical behavior of metal complexes $[Ru(bpy)_2(\mathbf{phen7T})]^{2+}$ and $[Ru(\mathbf{phen7T})_3]^{2+}$ (Figure S2 of the Supporting Information). Moreover, for polythiophene dendrimers, the redox species based on various conjugated sequences of α,α and α,β linkages are not easily resolved via the redox CV experiments.[6,7] Therefore, the thiophene dendron size effect cannot be inferred from our data at this point.

■ CONCLUSIONS

Two novel dendritic ligands, **phen3T** and **phen7T**, containing 1,10-phenanthroline coordination sites and thiophene dendrons, have been synthesized, along with the formation of four Ru(II) complexes of these oligothiophene dendron ligands. The absorption spectra, fluorescence properties, and redox behavior of the free ligands and of the Ru(II)−thiophene dendrimers have been studied, and a correlation between their structure and MLCT

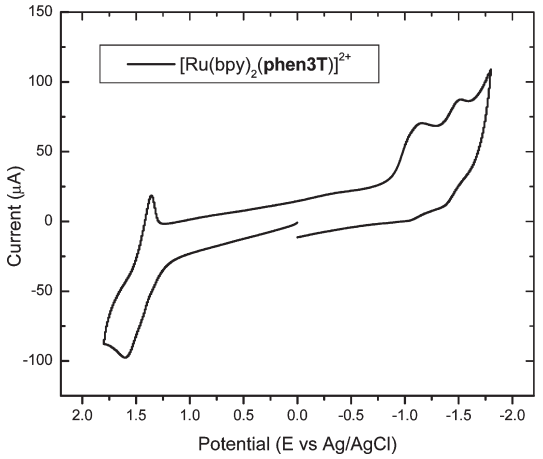

Figure 6. Cyclic voltammograms of the $[Ru(\mathbf{phen3T})_3]^{2+}$ complex with terthiophene dendron ligands. The rest of the CVs for the individual complexes appear as Supporting Information.

behavior was made. The Ru(II)−thiophene dendrimers exhibit unusually red-shifted MLCT emission of Ru(II)−polypyridine complexes. Moreover, these thiophene dendrimers exhibit very strong MLCT absorption and enhanced absorption in the UV region. They can be regarded as better light-harvesting species than either the generic Ru(II)−polypyridine complexes or all-polythiophene dendrimers.

EXPERIMENTAL SECTION

Materials. Thiophene dendrons (**Sn3T6COMe** and **7T6COMe**) were synthesized as we reported.[15] 4,7-Dibromo-1,10-phenanthroline was synthesized according to the literature procedure.[27] Other routes to thiophene-containing dendrimers have been considered. Spectroscopic-grade methylene chloride from Aldrich was used for spectral measurements. All other commercially available reagents were purchased from Aldrich and used as received. Silica gel (60 Å, 32−63 μm, standard grade) was purchased from Sorbent Technologies, Inc. (Atlanta, GA), and aluminum oxide (activated, neutral) was from Aldrich.

Instrumentation. NMR spectra were recorded on a General Electric QE-300 spectrometer operating at 300 MHz for ^{1}H and 75 MHz for ^{13}C nuclei. UV−vis spectra were recorded on an Agilent 8453 UV−visible spectrometer and fluorescence spectra on a PerkinElmer LS 45 luminescence spectrometer with a red sensitive photomultiplier tube (R928 from Hamamatsu). Cyclic voltammetry (CV) measurements were taken using a Bioanalysis BAS Epsilon Electroanalytical System with a three-electrode cell. The reference electrode was Ag/AgCl and calibrated against a ferrocene/ferrocenium couple. The working electrode was a glassy carbon, and the counter electrode was a Pt wire. The solutions contained ~0.5 mM metal complexes in CH_2Cl_2 with 0.05 M tetrabutylammonium hexafluorophosphate (TBAH) as the supporting electrolyte. Mass spectra were recorded on an ABI Voyager DE-STR (MALDI-TOF) using α-cyano-4-hydroxycinnamic acid as the matrix.

4,7-Bis[5,5″-bis(6-methoxyhexyl)[2,2′;3′,2″]terthiophen-5′-yl]-1,10-phenanthroline (phen3T). In a round-bottomed flask, 0.23 g of tributyl[5,5″-bis(6-methoxyhexyl)[2,2′;3′,2″]terthiophene-5′-yl]stannane (0.30 mmol), 33.8 mg of 4,7-dibromo-1,10-phenanthroline (0.10 mmol), 75 mg of $Pd(PPh_3)_4$, and 10 mL of DMF were charged. After three freeze−thaw cycles, the mixture was heated to 110 °C for 20 h under nitrogen. After cooling to room temperature, the reaction mixture was poured into water, extracted with CH_2Cl_2, and washed thoroughly with a NaF solution to remove tributyltin chloride. The organic layer was dried over Na_2SO_4 and concentrated. The residue was purified with a flash column using a 20:1 CH_2Cl_2/CH_3OH mixture as the eluent; 96 mg of pure product was obtained (85% yield): ^{1}H NMR ($CDCl_3$) δ 9.22 (d, 2H, J = 4.8 Hz), 8.46 (s, 2H), 7.73 (d, 2H, J = 4.2 Hz), 7.42 (s, 2H), 7.05 (d, 2H, J = 3.6 Hz), 6.98 (d, 2H, J = 3.9 Hz), 6.71 (m, 4H), 3.36 (m, 20H), 2.81 (t, 8H, J = 7.2 Hz), 1.69 (m, 8H), 1.58 (m, 8H), 1.40 (m, 16H); ^{13}C NMR ($CDCl_3$) δ 149.4, 147.5, 146.6, 146.0, 139.7, 135.9, 133.8, 133.7, 132.2, 131.2, 131.1, 127.6, 126.3, 125.5, 124.1, 123.9, 123.7, 123.1, 72.4, 58.1, 31.1, 31.0, 29.7, 29.6, 29.2, 28.5, 25.5.

2,3-Di[5,5″-di(6-methoxyhexyl)[2,2′;3′,2″]terthiophen-5′-yl]thiophene (7T6COMe). In a round-bottomed flask, tributyl[5,5″-bis(6-methoxyhexyl)[2,2′;3′,2″]terthiophen-5′-yl]stannane (2.3 g, 3.0 mmol), 2,3-dibromothiophene (242 mg, 1.0 mmol), 75 mg of $Pd(PPh_3)_4$, and 50 mL of DMF were charged. After three freeze−thaw cycles, the mixture was heated to 110 °C for 20 h under nitrogen. After cooling to room temperature, the reaction mixture was poured into water, extracted with CH_2Cl_2, and washed thoroughly with a NaF solution to remove tributyltin chloride. The organic layer was dried over Na_2SO_4 and concentrated. The residue was purified by column chromatography, eluting with a 1:1 hexane/diethyl ether mixture to give the yellow oil product (860 mg, 83%): ^{1}H NMR ($CDCl_3$) δ 7.27 (d, 1H, J = 6.0 Hz), 7.22 (s, 1H), 7.18 (s, 1H), 7.17 (d, 1H, J = 6.0 Hz), 6.95 (d, 1H, J = 2.1 Hz), 6.94 (d, 1H, J = 1.8 Hz), 6.88 (d, 1H, J = 3.3 Hz), 6.86 (d, 1H, J = 3.0 Hz), 6.66 (m, 4H), 3.36 (t, 8H, J = 6.3 Hz), 3.32 (s, 12H), 2.77 (t, 8H, J = 7.5 Hz), 1.67 (m, 8H), 1.57 (m, 8H), 1.38 (m, 16H); ^{13}C NMR ($CDCl_3$) δ 147.6, 147.4, 146.2, 146.0, 135.3, 135.0, 134.7, 133.0, 132.8, 132.4, 132.1, 132.0, 131.9, 131.8, 131.6, 131.2, 130.6, 129.8, 129.5, 127.8, 127.6, 126.5, 126.3, 125.1, 124.4, 124.3, 124.2, 73.0, 58.7, 31.7, 31.6, 30.2 (2), 29.7, 29.1, 29.0, 26.0.

Tributyl{2,3-di[5,5″-di(6-methoxyhexyl)[2,2′;3′,2″]terthiophen-5′-yl]thiophen-5-yl}stannane (Sn7T6COMe). Approximately 0.50 mL of *n*-butyllithium (2.5 M in hexane, 1.3 mmol) was added dropwise to a solution of 2,3-di[5,5″-di(6-methoxyhexyl)[2,2′;3′,2″]-terthiophen-5′-yl]thiophene (1.2 g, 1.2 mmol) in 20 mL of THF at −78 °C under N_2. After 30 min, 0.82 g of tributyltin chloride (0.42 g, 1.3 mmol) in 5.0 mL of anhydrous THF was added to the solution. The reaction mixture was then warmed to room temperature, stirred for an additional 3 h, and poured into a saturated $NaHCO_3$ solution. The mixture was extracted with CH_2Cl_2 and dried over $MgSO_4$ and the solvent evaporated. The residue was used for the next reaction without further purification: ^{1}H NMR ($CDCl_3$) δ 7.20 (s, 1H), 7.18 (s, 1H), 7.16 (s, 1H), 6.94 (m, 2H), 6.87 (m, 2H), 6.66 (m, 4H), 3.36 (t, 8H, J = 6.6 Hz), 3.32 (s, 12H), 2.77 (t, 8H, J = 7.2 Hz), 1.67 (m, 8H), 1.57 (m, 14H), 1.38 (m, 22H), 1.12 (m, 6H), 0.92 (t, 9H, J = 7.2 Hz).

4,7-Bis{2,3-Di[5,5″-di(6-methoxyhexyl)[2,2′;3′,2″]terthiophen-5′-yl]thiophen-5′-yl}-1,10-phenanthroline (phen7T) and Brphen7T. In a round-bottomed flask, 0.4 g of tributyl{2,3-di[5,5″-di(6-methoxyhexyl)[2,2′;3′,2″]terthiophen-5′-yl]thiophen-5-yl}stannane (**Sn7T6COMe**, 0.3 mmol), 33.8 mg of 4,7-dibromo-1,10-phenanthroline (0.1 mmol), 75 mg of $Pd(PPh_3)_4$, and 10 mL of DMF were charged. After three freeze−thaw cycles, the mixture was heated to 110 °C for 20 h under nitrogen. After cooling to room temperature, the reaction mixture was poured into water, extracted with CH_2Cl_2, and washed thoroughly with a NaF solution to remove tributyltin chloride. The organic layer was dried over Na_2SO_4 and concentrated. The residue was purified with a flash column using a 20:1 CH_2Cl_2/CH_3OH mixture as an eluent. Twelve milligrams of monocoupled byproduct **Brphen7T** (9.4% yield; R_f = 0.25) and 158 mg of **phen7T** (70% yield; R_f = 0.53) were obtained. **Brphen7T**: ^{1}H NMR ($CDCl_3$) δ 8.88 (d, 1H, J = 3.9 Hz), 8.45 (d, 1H, J = 9.0 Hz), 8.21 (d, 1H, J = 9.0 Hz), 7.87 (d, 1H, J = 7.5 Hz), 7.67 (d, 1H, J = 4.2 Hz), 7.48 (s, 1H), 7.32 (s, 1H), 7.27 (s, 1H), 6.96 (m, 2H), 6.90 (m, 2H), 6.67 (m, 4H), 6.59 (d, 1H, J = 7.5 Hz), 3.36 (t, 8H, J = 6.3 Hz), 3.32 (s, 12H), 2.77 (m, 8H), 1.67 (m, 8H), 1.57 (m, 8H), 1.38 (m, 16H); ^{13}C NMR ($CDCl_3$) δ 178.3, 148.3, 147.7, 147.5,

dx.doi.org/10.1021/cm200228p |*Chem. Mater.* 2011, 23, 3302–3311

146.3, 146.1, 140.4, 139.7, 137.1, 136.8, 136.6, 134.5, 134.2, 134.1, 133.9, 133.7, 132.4, 132.1, 132.0, 131.9, 131.7, 131.5 (2), 131.4, 130.8 (2), 130.0, 129.9, 128.7, 127.7, 127.6, 126.7, 126.5, 126.3, 124.5, 124.3, 124.1, 123.8, 123.7, 119.4, 113.4, 72.8, 58.5, 31.5, 31.4, 30.0 (2), 29.7, 29.5, 28.9, 25.8. **phen7T**: ^{1}H NMR ($CDCl_3$) δ 9.25 (d, 2H, J = 4.5 Hz), 8.48 (s, 2H), 7.76 (d, 2H, J = 4.5 Hz), 7.49 (s, 2H), 7.32 (s, 2H), 7.28 (s, 2H), 6.96 (d, 2H, J = 4.2 Hz), 6.95 (d, 2H, J = 3.9 Hz), 6.90 (d, 2H, J = 3.6 Hz), 6.87 (d, 2H, J = 3.0 Hz), 6.65 (m, 8H), 3.38−3.31 (m, 40H), 2.76 (m, 16H), 1.67 (m, 16H), 1.58 (m, 16H), 1.38 (m, 32H); ^{13}C NMR ($CDCl_3$) δ 149.9, 149.8, 147.6, 147.3, 146.9, 146.2, 146.0, 139.9, 137.3, 134.5, 134.2, 133.6, 133.5, 132.3, 132.0, 131.8, 131.7, 131.6, 131.4, 130.8, 129.9 (2), 127.7, 127.5, 126.5, 126.3, 126.0, 124.2, 124.2, 124.1, 123.7, 72.7, 58.5, 31.5, 31.4, 30.0 (2), 29.5, 28.9, 25.8.

Synthesis of [Ru(bpy)$_2$(phen3T)]$^{2+}$. $Ru(bpy)_2Cl_2\cdot 2H_2O$ (95 mg, 0.18 mmol) and **phen3T** (250 mg, 0.22 mmol) were added to wet DMF (10 mL) and heated at 120 °C for 4 days. After the mixture had been cooled to room temperature and an excess of solid NH_4PF_6 had been added, solvents were removed under reduced pressure. The residue was purified by using a column of neutral alumina, prepared with a 2:1 (v/v) toluene/acetonitrile mixture. The product was eluted using a 1:2 (v/v) toluene/acetonitrile mixture, after the solvent mixture had been gradually biased. The product [Ru(bpy)$_2$(**phen3T**)]$^{2+}$ was obtained as a red solid (185 mg, 56%): ^{1}H NMR ($CDCl_3$) δ 8.71 (s, 2H), 8.42 (m, 4H), 8.12 (d, 2H, J = 5.7 Hz), 7.96 (m, 4H), 7.83 (m, 4H), 7.65 (d, 2H, J = 5.7 Hz), 7.55 (s, 2H), 7.51 (m, 2H), 7.35 (m, 2H), 7.01 (d, 2H, J = 3.6 Hz), 6.96 (d, 2H, J = 3.6 Hz), 6.69 (m, 4H), 3.37 (t, 8H, J = 6.6 Hz), 3.32 (s, 6H), 3.31 (s, 6H), 2.77 (t, 8H, J = 7.5 Hz), 1.66 (m, 8H), 1.56 (m, 8H), 1.37 (m, 16H); ^{13}C NMR ($CDCl_3$) δ 156.6, 156.5, 151.8, 151.5, 151.3, 148.6, 148.2, 146.8, 140.7, 138.1, 136.5, 133.7, 133.3, 133.2, 130.8, 128.3, 128.2, 128.0, 127.1, 126.1, 124.5, 124.3, 124.2, 72.7, 58.5, 31.4 (2), 30.0, 29.9, 29.5, 28.8, 25.8; MALDI-TOF calcd for $C_{84}F_6H_{92}N_6O_4PRuS_6$ (M − PF_6) 1688.09 and $C_{84}H_{92}N_6O_4RuS_6$ (M − 2PF_6) 1543.13, found 1688 (M − PF_6), 1543 (M − 2PF_6).

Synthesis of [Ru(bpy)$_2$(phen7T)]$^{2+}$. $Ru(bpy)_2Cl_2\cdot 2H_2O$ (36.5 mg, 0.07 mmol) and **phen7T** (180 mg, 0.08 mmol) were added to wet DMF (5 mL) and heated at 120 °C for 4 days. After the mixture had been cooled to room temperature and an excess of solid NH_4PF_6 had been added, solvents were removed under reduced pressure. The residue was purified with a flash column [alumina neutral, 15:1 (v/v) $CHCl_3$/CH_3OH]. The product [Ru(bpy)$_2$(**phen7T**)]$^{2+}$ was obtained as a red oil (80 mg, 40%): ^{1}H NMR ($CDCl_3$) δ 8.81 (m, 4H), 8.76 (s, 2H), 8.34 (d, 2H, J = 5.4 Hz), 8.09 (m, 4H), 7.93 (m, 4H), 7.75 (d, 2H, J = 5.4 Hz), 7.62 (s, 2H), 7.58 (m, 2H), 7.43 (m, 2H), 7.32 (s, 2H), 7.27 (s, 2H), 6.95 (m, 4H), 6.88 (m, 4H), 6.66 (m, 8H), 3.37−3.30 (m, 40H), 2.77 (m, 16H), 1.65 (m, 16H), 1.56 (m, 16H), 1.37 (m, 32H); ^{13}C NMR ($CDCl_3$) δ 156.7 (2), 152.2, 151.5, 151.4, 148.3, 147.9, 147.5, 146.4, 146.1, 140.4, 138.3, 136.0, 134.5, 134.3, 134.1, 133.9, 133.4, 133.1, 132.5, 132.1, 132.0, 131.7, 131.4, 131.1, 130.9, 130.2, 128.2, 128.1, 127.8, 127.6, 126.6, 126.4, 125.0, 124.3, 124.2, 124.0, 72.7, 58.5, 31.4, 31.3, 29.9, 29.6, 29.5, 28.8, 25.8; MALDI-TOF calcd for $C_{144}H_{164}N_6O_8RuS_{14}$ (M − 2PF_6) 2656.87, found 2657 (M − 2PF_6).

Synthesis of [Ru(phen3T)$_3$]$^{2+}$. $RuCl_3\cdot 3H_2O$ (26 mg, 0.1 mmol) and **phen3T** (373 mg, 0.33 mmol) were added to wet DMF (10 mL) and heated at 120 °C for 4 days. After the mixture had cooled, a 4:1 (v/v) methanol/water mixture (20 mL) was added. The reaction mixture was heated to reflux for an additional 2 days. After the mixture had been cooled and an excess of solid NH_4PF_6 had been added, solvents were removed under reduced pressure. The residue was purified with a flash column [alumina neutral, 160:40:1 (v/v/v) CH_2Cl_2/ethyl acetate/CH_3OH]. [Ru(**phen3T**)$_3$]$^{2+}$ was obtained as a red oil (170 mg, 45%): ^{1}H NMR ($CDCl_3$) δ 8.76 (s, 6H), 8.29 (d, 6H, J = 6.0 Hz), 7.88 (d, 6H, J = 5.4 Hz), 7.57 (s, 6H), 7.05 (d, 6H, J = 3.6 Hz), 6.97 (d, 6H, J = 3.6 Hz), 6.70 (m, 12H), 3.36 (t, 24H, J = 6.3 Hz), 3.32 (s, 36H), 2.79 (t, 24H, J = 7.5 Hz), 1.68 (m, 24H), 1.57 (m, 24H), 1.38 (m, 48H); ^{13}C NMR ($CDCl_3$) δ 152.6, 148.4, 148.2, 146.7, 140.9, 136.6, 133.8, 133.5, 133.3, 133.2, 131.0, 128.3, 127.9, 127.0, 126.3, 126.0, 124.5, 124.2, 72.7, 58.4, 31.4, 31.3, 30.0, 29.9, 29.4, 28.8, 25.8; MALDI-TOF calcd for $C_{192}H_{228}N_6O_{12}RuS_{18}$ (M − 2PF_6) 3490.16, found 3491 (M − 2PF_6).

Synthesis of [Ru(phen7T)$_3$]$^{2+}$. $RuCl_3\cdot 3H_2O$ (8.6 mg, 0.03 mmol) and **phen7T** (250 mg, 0.12 mmol) were added to wet DMF (10 mL) and heated at 120 °C for 4 days. After the mixture had cooled, a 4:1 (v/v) methanol/water mixture (20 mL) was added. The reaction mixture was heated to reflux for an additional 2 days. After the mixture had been cooled and an excess of solid NH_4PF_6 had been added, solvents were removed under reduced pressure. The residue was purified with a flash column [alumina neutral, 20:1 (v/v) $CHCl_3$/CH_3OH]. [Ru(**phen7T**)$_3$]$^{2+}$ was obtained as a red oil (71.5 mg, 30%): ^{1}H NMR ($CDCl_3$) δ 8.76 (s, 6H), 8.00 (m, 6H), 7.79 (m, 6H), 7.66 (m, 6H), 7.55 (m, 6H), 7.28 (m, 6H), 6.95 (m, 12H), 6.88 (m, 12H), 6.66 (m, 24H), 3.35 (m, 120H), 2.76 (s, 48H), 1.62 (m, 48H), 1.55 (m, 48H), 1.37 (m, 96H); MALDI-TOF calcd for $C_{372}H_{444}N_6O_{24}RuS_{42}$ (M − 2PF_6) 6831.37, found 6832 (M − 2PF_6).

■ ASSOCIATED CONTENT

Supporting Information. Correction file, uncorrected and corrected emission spectra, and cyclic voltammograms of model complexes. This material is available free of charge via the Internet at http://pubs.acs.org.

■ AUTHOR INFORMATION

Corresponding Author
*E-mail: radvincula@uh.edu.

■ ACKNOWLEDGMENT

We acknowledge the Robert A. Welch Foundation (E-1551 for S.D. and R.C.A.; E-621 for R.Z. and R.P.T.). R.Z. and R.P.T. also thank the Division of Chemical Sciences, Geosciences, and Biosciences, Office of Basic Energy Sciences of the U.S. Department of Energy through Grant DE-FG02-07ER15888.

■ REFERENCES

(1) (a) Setif, P.; Bottin, H.; Brettel, K. *Current Research in Photosynthesis*; Baltscheffsky, M., Ed.; Kluwer: Dordrecht, The Netherlands, 1990; Vol. II, p 539. (b) Holzwarth, A. R.; Hachnel, W.; Ratajczak, R.; Bittersmann, E.; Schatz, G. H. *Current Research in Photosynthesis*; Baltscheffsky, M., Ed.; Kluwer: Dordrecht, The Netherlands, 1990; Vol. II, p 611.

(2) Newkome, G. R.; Moorefield, C.; Vögtle, F. *Dendrimers and Dendrons*; Wiley-VCH: Weinheim, Germany, 2001; and references cited therein.

(3) (a) Kalyanasundaram, K. *Photochemistry of Polypyridine and Porphyrin Complexes*; Academic Press: San Diego, 1992. (b) *Organic and Inorganic Photochemistry*; Ramamurthy, V., Schanze, L. S., Eds.; Marcel Dekker: New York, 1998.

(4) (a) Balzani, V.; Campagna, S.; Denti, G.; Juris, A.; Serroni, S.; Venturi, M. *Acc. Chem. Res.* **1998**, *31*, 26–34. (b) Plevoets, M.; Vögtle, F.; DeCola, L.; Balzani, V. *New J. Chem.* **1999**, *23*, 63–69.

(5) (a) Yamamoto, T.; Yoneda, Y.; Kizu, K. *Macromol. Rapid Commun.* **1995**, *16*, 549–556. (b) Watts, R. J.; Crosby, G. A. *J. Am. Chem. Soc.* **1972**, *94*, 2606–2614.

(6) Xia, C.; Fan, X.; Locklin, J.; Advincula, R. C. *Org. Lett.* **2002**, *4*, 2067–2070.

(7) (a) Xia, C.; Fan, X.; Locklin, J.; Advincula, R. C.; Gies, A.; Nonidez, W. *J. Am. Chem. Soc.* **2004**, *126*, 8735–8743. (b) Sriwichai, S.; Baba, A.; Deng, S.; Huang, C.; Phanichphant, S.; Advincula, R. C. *Langmuir* **2008**, *24*, 9017–9023.

(8) Ma, C. Q.; Mena-Osteritz, E.; Debaerdemaeker, T.; Wienk, M. M.; Janssen, R. A.; Bäuerle, P. *Angew. Chem., Int. Ed.* **2007**, *46*, 1679–1683.
(9) Harpham, M. R.; Süzer, Ö.; Ma, C. Q.; Bäuerle, P.; Goodson, T., III. *J. Am. Chem. Soc.* **2009**, *131*, 973–979.
(10) Mitchell, W. J.; Kopidakis, N.; Rumbles, G.; Ginley, D. S.; Shaheen, S. E. *J. Mater. Chem.* **2005**, *15*, 4518–4528.
(11) Kopidakis, N.; Mitchell, W. J.; Van de Lagemaat, J.; Ginley, D. S.; Rumbles, G.; Shaheen, S. E.; Rance, W. L. *Appl. Phys. Lett.* **2006**, *89*, 103524(1)–103524(3).
(12) Negishi, N.; Ie, Y.; Taniguchi, M.; Kawai, T.; Tada, H.; Kaneda, T.; Aso, Y. *Org. Lett.* **2007**, *9*, 829–832.
(13) Wong, W. W. H.; Ma, C. Q.; Pisula, W.; Yan, C.; Feng, X.; Jones, D. J.; Müllen, K.; Janssen, R. A. J.; Bäuerle, P.; Holmes, A. B. *Chem. Mater.* **2010**, *22*, 457–466.
(14) Mishra, A.; Ma, C. Q.; Baeuerle, P. *Chem. Rev.* **2009**, *109*, 1141–1276.
(15) (a) Takagi, K.; Torii, C.; Yamashita, Y. *J. Polym. Sci., Part A: Polym. Chem.* **2009**, *47*, 3034–3044. (b) Martín-Zarco, M.; Toribio, S.; García-Martínez, J.; Rodríguez-López, J. *J. Polym. Sci., Part A: Polym. Chem.* **2009**, *47*, 6409–6419.
(16) Loren, J. C.; Siegel, J. S. *Angew. Chem., Int. Ed.* **2001**, *40*, 754–757.
(17) Crosby, G. A.; Elfring, W. H. *J. Phys. Chem.* **1976**, *80*, 2206–2211.
(18) Damrauer, N. H.; Boussie, T. R.; Devenney, M.; McCusker, M. K. *J. Am. Chem. Soc.* **1997**, *119*, 8253–8268.
(19) McClenaghan, N. D.; Passalacqua, R.; Loiseau, F.; Campagna, S.; Verheyde, B.; Hameurlaine, A.; Dehaen, W. *J. Am. Chem. Soc.* **2003**, *125*, 5356–5365.
(20) (a) Crosby, G. A. *Acc. Chem. Res.* **1975**, *8*, 231–238. (b) Meyer, T. J. *Acc. Chem. Res.* **1989**, *22*, 163–170.
(21) Jaffe, H. H.; Orchin, M. *Theory and Applications of Ultraviolet Spectroscopy*; Wiley, Inc.: New York, 1962.
(22) Juris, A.; Balzani, V.; Barigelletti, F.; Campagna, S.; Belser, P.; von Zelewsky, A. *Coord. Chem. Rev.* **1988**, *84*, 85–277.
(23) Bernhard, S.; Barron, J. A.; Houston, P. L.; Abruña, H. D.; Ruglovksy, J. L.; Gao, X.; Malliaras, G. G. *J. Am. Chem. Soc.* **2002**, *124*, 13624–13628.
(24) Zong, R.; Thummel, R. P. *J. Am. Chem. Soc.* **2004**, *126*, 10800–10801.
(25) Vögtle, F.; Plevoets, M.; Nieger, M.; Azzellini, G. C.; Credi, A.; De Cola, L.; De Marchis, V.; Venturi, M.; Balzani, V. *J. Am. Chem. Soc.* **1999**, *121*, 6290–6298.
(26) Vögtle, F.; Gestermann, S.; Hesse, R.; Schwierz, H.; Windisch, B. *Prog. Polym. Sci.* **2000**, *25*, 987–1041.
(27) Graf, G. I.; Hastreiter, D.; da Silva, L. E.; Rebelo, R. A.; Montalban, A. G.; McKillop, A. *Tetrahedron* **2002**, *58*, 9095–9100.